Journal of Dentistry 85 (2019) 64–72

Contents lists available at ScienceDirect

Journal of Dentistry

journal homepage: www.elsevier.com/locate/jdent

Altering of optical and mechanical properties in high-translucent CAD-CAM resin composites during aging

Nicoleta Ilie

Department of Operative Dentistry and Periodontology, University Hospital, Ludwig-Maximilians-Universität München, Goethestr. 70, D-80336, Munich, Germany

ARTICLE INFO

Keywords:
CAD-CAM resin based composites
Aging
Optical properties
Micromechanical properties
Edge chipping resistance parameters

ABSTRACT

Objectives: This study was aimed to monitor the alteration of the optical and mechanical properties of high-translucent CAD-CAM resin composites (HTRCs) during aging. Corrections for the measured transmitted irradiance are proposed.

Methods: Individual sets (n = 6) of plane-parallel test specimens (0.5-, 2- and 4-mm) of seven HTRCs were prepared. The optical properties (absorbance, transmittance, reflectance, linear absorption coefficient, and transmitted irradiance) were assessed by regular spectrometric testing methodologies and were corrected to account for light reflection. Several edge chipping resistance parameters (edge force at different edge distances, edge chip resistance), as well as mechanical parameters obtained from depth-sensing indentation (Vickers hardness, indentation modulus, creep, elastic and plastic indentation work), were considered. Aging involved storage for two weeks in artificial saliva at 37 °C, followed by thermal aging (10,000 thermocycles, 5 °C–55 °C) and storage in alcohol/water solution, employing non-aged specimens as a reference. Filler size and shape were analyzed by scanning electron microscopy.

Results: Reflectance varied from 11% to 27% and was altered during aging. Linear absorption coefficients of 0.281 mm^{-1} to 0.369 mm^{-1} were obtained for non-aged specimens, with very low changes during aging. A difference between the true and measured irradiance was identified to decrease exponentially with the specimen's thickness. The impact of HTRC was stronger than the impact of aging.

Conclusions: Reflectance determined by spectrometric analysis was identified as a possible criterion to estimate surface degradation during aging. Corrections for thin and translucent specimens are needed when determining transmitted irradiance through restorations. Depth-sensing indentation was evidenced as the most discriminatory testing methodology for aging, but the results do not correlate with the edge chipping resistance parameters.

1. Introduction

High-translucent computer-aided design and computer-aided manufacturing (CAD-CAM) resin composites (HTRCs) are the most recently launched CAD-CAM dental restoratives. They broaden the spectrum of CAD-CAM resin composites to enhance esthetics. Concomitantly, the higher translucency should allow for adhesive cementation via dual or simply light cure luting resin composites. Thus far, the transmitted light through this material category and aging behavior have been insufficiently characterized.

On comparing CAD-CAM resin composites with CAD-CAM glass-ceramics/ceramics, the former may offer significant advantages related to their machinability and intraoral reparability [1]. However, their mechanical properties are presented as heterogeneous in the literature. Monolithic CAD-CAM resin composites have demonstrated good fatigue resistance that is comparable to that of lithium disilicate glass-ceramic [2] or that is even better than leucite glass-ceramic materials [3]. Parameters such as flexural strength [1,4], flexural modulus [1,4] fracture toughness [1] and hardness [4] were found to be higher in glass-ceramics. Compared with conventional resin composites, enhanced hardness was identified in CAD-CAM resin composites [5]. Owing to the high pressure and high temperature polymerization, no monomer elution was detected from CAD/CAM resin composites [5], but their mechanical properties were shown to degrade during aging [1,6].

From a clinical perspective, a commonly observed failure in brittle restoratives is chipping. This issue is investigated in vitro by edge chipping resistance tests that have been previously established for technical ceramics. Edge chipping resistance tests for dental materials are now specified in several standards [7–9]. They have proven to be

E-mail address: nilie@dent.med.uni-muenchen.de.

https://doi.org/10.1016/j.jdent.2019.05.015
Received 14 January 2019; Received in revised form 7 May 2019; Accepted 8 May 2019

discriminatory testing methodologies [7] in characterizing the human tooth structure [10], restoratives such as polymethylmethacrylate (PMMA)-based composites [11], CAD/CAM [12] and light-cured resin composites [11,13–15], as well as dental ceramics [12,13,16]. Principally, an edge chipping test consists of an indentation test performed close to the sample edge. The test records the critical load needed to create a chip. The dependency of the force distance data has been identified to be nonlinear [7]. Simplified edge chipping resistance tests limit the distance variation to a single value (0.5 mm) that is considered a clinically relevant situation in which chipping is induced [14]. Test-relevant parameters such as the type and sharpness of the indenter have been evidenced to have a significant impact on the measured parameters [7].

The aim of the present study was to monitor various optical and mechanical properties of modern high-translucent CAD/CAM resin composites during aging. Optical properties (absorbance, transmittance, reflectance, linear absorption coefficient, transmitted irradiance) are thereby assessed by regular spectrometric testing methodologies and corrected to account for light reflection, as previously proposed in the literature [17]. To allow the determination of true transmitted irradiance, an extension of the Watts and Cash theory [17] was proposed. Furthermore, the mechanical behavior is described by evaluating several edge chipping resistance parameters, accounting for the nonlinear dependency of the *chipping force-distance from the edge* data [7] and mechanical parameters obtained from depth-sensing indentation (Vickers hardness, HV; indentation modulus, Y_{HU}; creep, Cr; elastic, W_{elast}; total W_{tot} (= elastic + plastic) indentation work).

The null hypotheses were as follows: a) HTRC and b) aging (involving storage for two weeks in artificial saliva at 37 °C, additional thermal aging—10,000 thermo cycles between 5 °C and 55 °C—and storage in a 75 vol. % alcohol/water solution, employing no-aged specimens as a reference) had no effect on the tested optical and mechanical parameters.

2. Materials and methods

The effect of aging on representative high-translucent CAD-CAD resin composites (Table 1) was addressed using the optical properties, edge chipping resistance and micromechanical properties.

Individual specimen sets (n = 6) of plane-parallel solid test specimens were prepared for each test and material. Edge chipping resistance and micromechanical properties were measured on 4-mm-thick specimens. Optical properties were assessed on three different thicknesses (0.5, 2 and 4 mm). The specimen's width and depth corresponded to the dimensions of the individual CAD-CAM blocks, which varied between (13.9–14.7) mm and (10.6–14.6) mm, respectively.

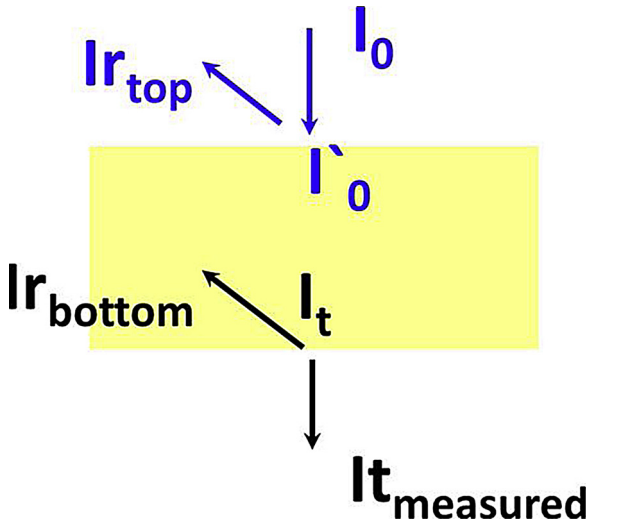

Fig. 1. flat, planar surface of a CAD-CAM resin composite receiving an incident light intensity I_0 normal to the surface. The reflected light intensity on the top surface is Ir_{top}. The light intensity immediately subsurface is $I_0` = I_0 - Ir_{top}$. This light is attenuated when travelling through the material of a given thickness to I_t and reflected at the bottom surface of the specimen (Ir_{bottom}). The measured light irradiance $It_{measured}$ is then $It_{measured} = I_t - Ir_{bottom}$.

CAD/CAM blocks were cut using a low-speed diamond saw (Isomet low-speed saw; Buehler, Germany) under water cooling, than ground with SiC paper till Grit 4000. The thickness of each specimen was determined at two points using a digital micrometer screw gauge (Mitutoyo, Kawasaki, Japan). Thickness tolerance was set to 0.05 mm. Specimens belonging to the control group received no treatment. For aging, the same specimens were stored for two weeks in artificial saliva at 37 °C, followed by thermal aging. This storage step was abbreviated TC and corresponded to 10,000 thermocycles between 5 °C and 55 °C at a dwell time of 30 s per temperature and a transfer time of 5 s between bathes. The subsequent storage in 75 vol. % alcohol/water solution for two days is abbreviated ALC.

2.1. Optical properties

Incident (I_0) and transmitted irradiance ($I_{t,\ measured}$, Fig. 1) through 0.5-mm-, 2-mm- and 4-mm-thick specimens (n = 6) of each material-storage combination were assessed on a laboratory-grade National Institute of Standards and Technology (NIST)-referenced USB4000

Table 1
Materials, abbreviations, manufacturer, shade and LOT number for the CAD/CAM restoratives.

Code	Material	Manufacturer	Shade	LOT	Monomer	Filler		
						composition	Wt%	Vol%
BC	Brilliant Crios	Coltene	A3 HT	I35186	methacrylates	SiO_2, barium glass	70.7	51.5
CS	Cerasmart	GC	A3 HT	1702011	Bis-MEPP, UDMA, DMA	SiO_2, barium glass	71	n.a.
GB	Grandio Blocs	Voco	A3 HT	1709591	methacrylates	n.a.	86	n.a.
LC	Luxacam Composite	DMG	A3	769515	methacrylates	SiO_2-glass	70	n.a.
LU	Lava Ultimate	3 M	A3 HT	N933699	Bis-GMA, UDMA, Bis-EMA, TEGDMA	SiO_2, ZrO_2, aggregated ZrO_2/SiO_2 cluster	80	n.a.
SB	Shofu Block HC	Shofu	A3 HT	071601	UDMA, TEGDMA	SiO_2, silicate, zirconium silicate	61	n.a.
TC	Tetric CAD	Ivoclar Vivadent	A3 HT	W93631	Bis-GMA Bis-EMA TEGDMA UDMA	Ba-Al-SiO_2- glass, SiO_2	71.1	n.a.

Abbreviations: Bis-EMA = ethoxylated bisphenol A dimethacrylate, Bis-GMA = bisphenol A glycol dimethacrylate, Bis-MEPP = 2,2-bis(4-methacryloxyethoxyphenyl)propane, DMA = dimethacrylate, TEGDMA = Triethylene glycol dimethacrylate, UDMA = Urethane dimethacrylate, SiO_2 = silicon oxide (silica), ZrO_2 = zirconium oxide.

Spectrometer. Therefore, a blue-violet LED light curing unit (LCU) (Bluephase Style; Ivoclar Vivadent, Schaan, Liechtenstein) was employed. The incident irradiance (the irradiance reaching the specimen's surface) was determined on six occasions by applying the LCU directly to the sensor.

The transmitted irradiance was measured by positioning the specimens between the LCU and sensor. The CAD/CAM specimens were aligned centered on the round detector of the spectrometer, which had a diameter of 3.9 mm. Consequently, the irradiance reaching this area was considered. The miniature fiber optic USB4000 Spectrometer employs a 3648-element Toshiba linear Charge-coupled Device (CCD) array detector and high-speed electronics (Ocean optic, Largo, FL, USA). The spectrometer was calibrated using an Ocean Optics' NIST-traceable light source (300–1050 nm). The system uses a CC3-UV Cosine Corrector (Ocean optic, Largo, FL, USA) to collect radiation over a 180° field of view, thus mitigating the effects of optical interference associated with light collection sampling geometry. Irradiance at a wavelength range of 360–540 nm was individually collected at a rate of 16 records/s. The sensor was triggered at 20 mW.

The integrated optical transmission (T) was determined for each material and aging condition. (T) is defined as the ratio of the transmitted irradiance (radiant power) to the incident irradiance: $T = I(d)/I_0$, where I(d) is the irradiance after the beam of light passes through the specimen of thickness d, and I_0 is the irradiance of the incident light. The data were converted to absorbance values (Absorbance (A) = $-\log(T) = -\log(I(d)/I_o)$) and were corrected according to Watts and Cash [17] to account for light reflection. Therefore, the measured light absorption, which is defined by Watts and Cash as apparent light absorption, A' [17], was plotted against the specimen thickness, and the positive intercept (C) at a specimen thickness of 0 mm was calculated. This allows determination of the surface reflection ratio (R), the ratio of reflected light to incident light: $R = (I_r/I_0) = 1 - 10^{-C}$. True A values were then obtained as A = A' - C [17].

The (decadic) linear absorption coefficient was determined from the relationship between the true absorbance (A) to path length (d) $A = a\,x\,d$, according to the Beer-Lambert law for light attenuation within a medium.

Based on the considerations of Watts and Cash [17], an extension of their correction method is proposed, allowing the calculation of the true value of the transmitted irradiance through a material from the measured spectrometric data. This is an important prerequisite to assess if sufficient light reaches the underlying light or dual-curing luting material, when luting indirect restoratives.

Watts and Cash theory allows determining the surface reflection ratio (R) [17]. Because the analyzed materials are solids and are not wetting the sensor, reflection will occur on the top and bottom surfaces of the specimen (Fig. 1). Accordingly, the surface reflection ratio R is:

$R = R_t + R_b$, with

R_t = reflection ratio at the top surface (= Ir_{top}/I_0; Ir_{top} = reflected irradiance at the top surface; I_0 = incident irradiance) and

R_b = reflection ratio at the bottom surface (= Ir_{bottom}/I_t; Ir_{bottom} = reflected irradiance at the bottom surface; I_t = true transmitted irradiance).

Considering that $Ir_{top}/I_0 = Ir_{bottom}/I_t$, the surface reflection ratio for the specimen's top and bottom is:

$$R_t = R_b = R/2 \quad (1)$$

As described in Fig. 1, $Ir_{bottom} = I_t - It_{measured}$ (2), with $It_{measured}$ = measured transmitted irradiance

$$R_b = Ir_{bottom}/I_t = (I_t - It_{measured})/I_t = 1 - (It_{measured}/I_t) \quad (3)$$

The true transmitted irradiance can be calculated after rearranging Eq.s (1) and (3):

$$I_t = I_{t,\,measured}/(1\text{-}R/2). \quad (4)$$

2.2. Edge chipping resistance

Edge chipping was determined using a universal testing machine (Zwick/Roell Z 2.5; AST GmbH, Ulm, Germany). The edge distance *d* was carefully set to a prescribed value (0.20 mm, 0.30 mm, 0.40 mm and 0.50 mm) prior to each chip test. Force, *F*, was gradually applied in the displacement control at 0.5 mm/min until fracture. When a chip popped off, a sudden force drop off was detected, and the peak load was recorded. The used Vickers diamond indenter (diamond right pyramid with a square base and an angle $\alpha = 136°$ between opposite faces at the vertex) was extracted automatically at the 10% force drop off. Usually, twenty-four to twenty-eight chips were made per material-aging combination.

The dependency between the chipping force, *F*, and distance from the edge, *d*, allows characterization of the edge chipping resistance by following parameters:

- Critical load needed to create a chip at an arbitrary distance (d) away from the edge; d = 0.5 mm is considered a clinically relevant distance, as proposed by Watts et al. [14] and included in the ASTM WK45217 [8].
- Edge chip resistance, R_{eA}, defined as the ratio of the force to distance, with units of N/mm [7,9].

2.3. Micromechanical properties

Measurements were made using an automatic micro hardness indenter (Fischerscope H100C; Fischer, Sindelfingen, Germany) on 4-mm-thick specimens (n = 6) summarizing 36 single indentations for each material-aging condition.

The test procedure was carried out force-controlled, where the test load increased and decreased with constant speed between 0.4 mN and 500 mN. The load and penetration depth of the indenter were continuously measured during the load-unload hysteresis. Universal hardness was defined as the test force divided by the apparent area of indentation under the applied test force. From a multiplicity of measurements stored in a database supplied by the manufacturer, a conversion factor between Universal hardness and Vickers hardness (HV) was calculated and input into the software. The indentation modulus (Y_{HU}) was calculated from the slope of the tangent of the indentation depth curve at the maximum force. Furthermore, the mechanical work, W_{total}, indicated during the indentation procedure was considered. W_{total} is only partly consumed as the plastic deformation work, W_{plast}. During removal of the test force, the remaining part is set free as the work of the elastic reverse deformation $W_{elastic}$. According to the definition of mechanical work as $W = \int Fdh$ (F = load; h = indentation depth) and considering the force variation during load and discharge, the total mechanical work and its components are calculated. In addition, the change in the indentation depth at a constant test force (F = 500 mN) was measured, allowing calculation of the relative change in the indentation depth. This is a value for the creep (Cr) of the material.

2.4. Scanning electron microscopy (SEM)

One specimen of each non-aged material was selected for SEM analysis (Zeiss Supra 55 V P, Oberkochen, Germany). Specimens were unsputtered, while the images were taken using a backscatter signal (RBSD).

2.5. Statistical analysis

The Shapiro–Wilk test verified the normal distribution of the data. Multivariate analysis (general linear model) assessed the effects of various parameters, as well as their interaction terms on the measured mechanical and optical parameters. The partial eta-squared statistic

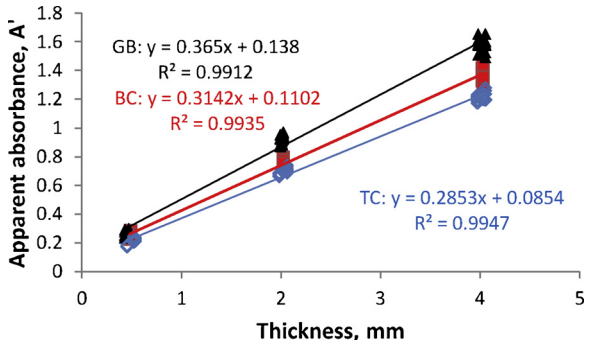

Fig. 2. Linear regression plot of the apparent blue light absorption, A`, versus specimen thickness (n = 6 for each thickness) exemplified on non-aged specimens made of the materials GB, BC and TC (y = αx + C; α = linear absorption coefficient). (For interpretation of the references to colour in this figure legend, the reader is referred to the web version of this article).

reports the practical significance of each term based on the ratio of the variation accounting for the effect. Larger values of partial eta-squared indicate a greater amount of variation accounted for by the model effect, to a maximum of 1. The correlation among parameters has been employed by Pearson correlation analysis. In all statistical tests, p-values < 0.05 were considered statistically significant when using SPSS Inc. (Version 24.0; Chicago, IL, USA).

3. Results

3.1. Optical properties

The absorbance vs. specimen thickness variation is illustrated graphically in Fig. 2 for a representative HTRC. The tabulated linear regression parameters and intercept "C" are presented in Table 2 for all materials and aging conditions, and the fit to a linear plot is highly statistically significant in every case ($p < 0.05$) and for all materials.

The surface reflection ratio, calculated in accordance with Watts and Cash equations [17] varies from 17% to 27% among the materials investigated under dry conditions, from 14% to 24% after thermocycling and from 11% to 19% after aging in alcohol.

Table 2
Optical transmission and reflection parameters (CI = Coefficient of determination for the linear absorption coefficient, $R^2 > 0.99$, calculated in accordance with Watts and Cash equations [17].

aging	Cod	Intercept (C)	surface reflection ratio (R, %)	95% CI of the linear absorption coefficient, mm^{-1}
no treatment (reference)	BC	0.101	0.210	0.313 ÷ 0.323
	CS	0.071	0.150	0.301 ÷ 0.309
	GB	0.134	0.270	0.360 ÷ 0.376
	LC	0.128	0.250	0.316 ÷ 0.323
	LU	0.118	0.240	0.358 ÷ 0.368
	SB	0.096	0.200	0.304 ÷ 0.313
	TC	0.083	0.170	0.276 ÷ 0.285
Thermal aging TC	BC	0.078	0.160	0.317 ÷ 0.327
	CS	0.068	0.140	0.292 ÷ 0.299
	GB	0.117	0.240	0.357 ÷ 0.368
	LC	0.119	0.240	0.307 ÷ 0.315
	LU	0.118	0.240	0.361 ÷ 0.370
	SB	0.086	0.180	0.305 ÷ 0.312
	TC	0.064	0.140	0.283 ÷ 0.289
Alcohol ALC	BC	0.061	0.130	0.323 ÷ 0.329
	CS	0.053	0.110	0.292 ÷ 0.301
	GB	0.089	0.190	0.357 ÷ 0.368
	LC	0.086	0.180	0.313 ÷ 0.320
	LU	0.090	0.190	0.361 ÷ 0.370
	SB	0.052	0.110	0.316 ÷ 0.321
	TC	0.062	0.130	0.281 ÷ 0.288

The linear absorption coefficient was highest in GB ($0.369\ mm^{-1}$) and lowest in TC ($0.281\ mm^{-1}$) in non-aged specimens, with very low changes during aging, as evidenced by a slightly but significant decrease after thermocycling in CS and LC and a slightly but significant increase after aging in alcohol in SB (Table 2; 95% CI for the linear absorption coefficient).

The true and measured transmitted irradiance is presented in Fig. 3 for all CAD-CAM resin composites and thicknesses, prior to aging the materials. The difference between the true and measured values (ΔIt = It (true) – It (measured)) decreased exponentially with the thickness. ΔIt correlated moderately with the linear absorption coefficient (Pearson correlation coefficient = - 0.567, $p < 0.01$) in thin specimens (0.5 mm thickness). The correlation was weaker in 2-mm increments (- 0.338, $p < 0.05$) and was no longer significant in 4-mm increments.

3.2. Edge chipping resistance

All of the analyzed parameters—edge distance, material and aging, as well as their binary but not ternary, interaction products—exerted a significant ($p < 0.001$) effect on the edge force. The highest influence was exerted by the parameter edge distance ($p < 0.001$; partial eta squared $\eta P^2 = .688$), followed by material (.357) and aging (.138). Chipping force vs. edge distance is illustrated graphically in Fig. 4a–c for all materials and aging conditions. Non-aged specimens (Fig. 4a) presented heterogeneous critical edge chipping forces at lower edge distances (0.2 mm). For larger distances, two homogeneous material groups are identified, with LU, GB, and SB ($p = 0.997$ within the group for d = 0.5 mm) presenting lower critical edge chipping forces ($p < 0.001$) than LC, CS, BC and TC ($p = 0.942$). The difference between the groups is accentuated with the edge distance (Fig. 4a). Considering all materials at each chipping distance, the immersion in alcohol additionally to thermal cycling induced similar chipping forces as the thermal-cycling process alone (in ascending order of the chipping distance, p = 0.570; 0.864; 0.732 and 0.802). Similarly, no significant difference was identified between thermal cycling and no aging in chipping distances of 0.2 mm ($p = 0.195$) and 0.3 mm ($p = 0.059$), while chipping forces were lower after thermal cycling at chipping distances of 0.4 mm ($p = 0.009$) and 0.5 mm ($p = 0.03$). Immersion in alcohol reduced the chipping force compared with no aging conditions (in ascending order of the chipping distance p = 0.017; 0.015; 0.050 and < 0.001).

Fig. 5 summarizes the clinically relevant chipping distance of 0.5 mm. The critical force to induce a chip at a 0.5-mm edge distance was influenced by a decreased ranking of the parameter *material* ($p < 0.001$; $\eta_P^2 = .430$), the interaction term *material x aging* (.282) and *aging* (.255). A similar effect was also identified for the measured parameter *edge chip resistance* ($p < 0.001$, $\eta_P^2 = .317$, .141 and .100, respectively; Fig. 6).

3.3. Micromechanical properties

All analyzed parameters—material and aging, as well as their binary interaction product—exerted a significant ($p < 0.001$) and strong effect on the measured micromechanical properties (Table 3, Fig. 7).

An excellent correlation was identified between the filler weight % and micromechanical properties (Pearson's correlation coefficient = .915 (HM) to -.704 (Cr)). The correlation coefficient increased with the aging procedure (.944 (HM) to -.738 (Cr)). The filler shape and morphology are presented in the scanning electron microscopy records in Fig. 8.

The correlation among parameters HM, HV, Y_{HU}, W_{elast} and W_{tot} was also very high (.90 to .99). The correlation of the abovementioned parameters with Cr was slightly lower (-.704 to -.758). Notably, an inverse correlation was identified among the parameters HM, HV, and Y_{HU} and parameters W_{elast}, W_{tot} and Cr.

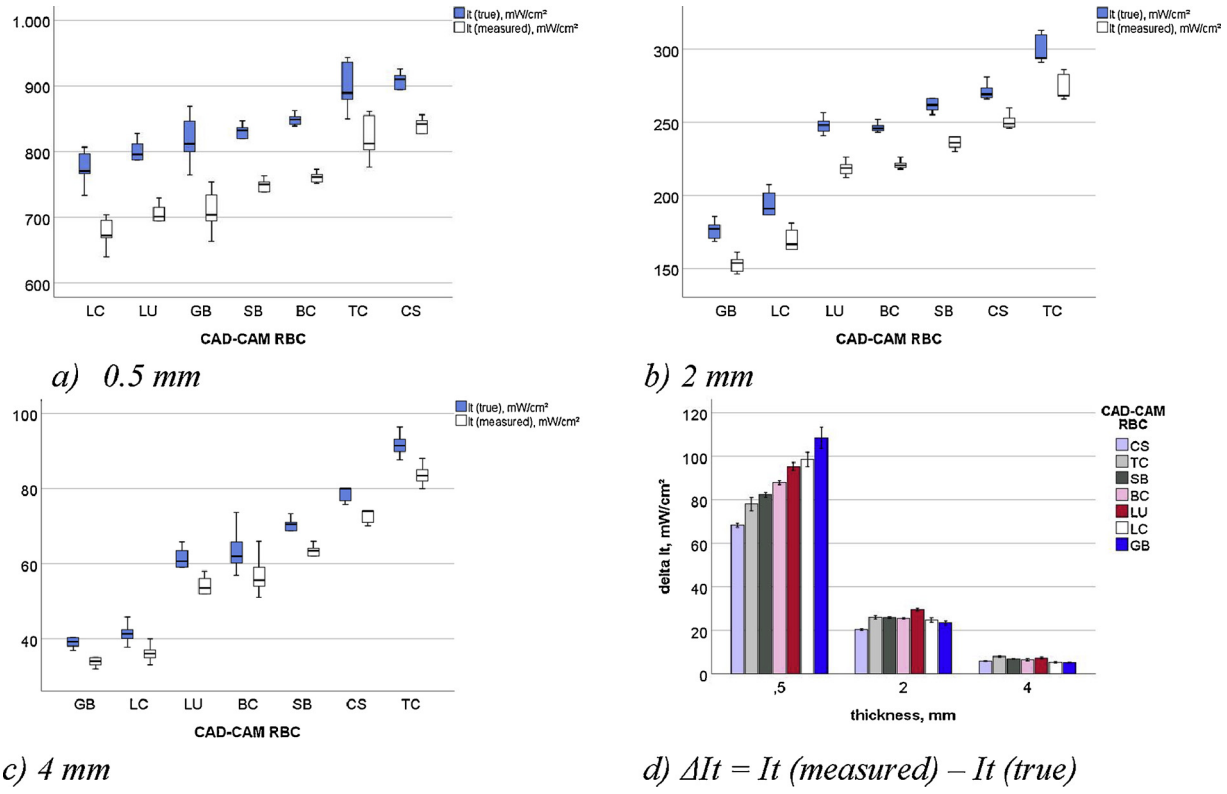

Fig. 3. True and measured transmitted irradiance through CAD-CAM resin composites of a) 0.5 mm, b) 2 mm; c) 4 mm thickness; d) Difference between true and measured transmitted irradiance as a function of material and thickness.

No correlation was identified among the micromechanical parameters and parameters calculated in the edge chipping resistance test.

4. Discussion

When curing a luting resin composite through indirect restorations, light may be reflected, absorbed, scattered or transmitted. The attenuating effects of light, when passing through matter, such as scattering or reflection, are summarized in optics together with the absorption under the term extinction or absorbance and depend on the material, angle of incidence and frequency of the light. The absorbance measured by regular spectrometric testing methodologies must account for light reflection, as previously shown [17]. The present study identified a substantial surface reflectance that varies from 11% to 27%. Considering that the incident light was constant and perpendicular to the material surface, the reflection of light, when incident on the interface between different optical media (air and CAD/CAM resin composite), can be described by the Fresnel equation as: $R = [(n_1\text{-}n_2)/(n_1+n_2)]^2$, where n_1 is the refractive index of air (= 1.00028) and n_2 is the refractive index of the CAD/CAM resin composite. The analyzed materials basically comprise a methacrylate polymer matrix (n = ca. 1.55) and inorganic fillers such as fused silica (n = 1.4527), barium glass (n = 1.5100) and zirconium oxide (n = 2.1326) (Table 1). At an estimated average CAD/CAM resin composite refractive index of 1.5 and an extension of this value up to 1.8 to allow for diversity in chemical composition, the reflectance, as calculated according to the Fresnel equation, will amount 4–8.16%. This result diverges from the calculated reflectance values that were highest in GB (27% in no aged; 24% in TC and 19% in ALC) and lowest in CS (15% no aged; 14% TC and 11% ALC), while decreasing with aging. Considering that all analyzed specimens have been polished following an identical protocol, it is apparent that a difference in reflectance or reflection ratio (= fraction of incident radiance that is reflected at the interface) among theoretically calculated and measured values or among different materials may be related, in addition to the index of refraction of the material, also to the material's ability to be polished and, consequently, the filler size, distribution, geometry and volume fraction [18]. The polishing capacity of dental resin composites has been shown to improve with smaller particle sizes and higher filler loading [19]. The former was confirmed in the analyzed materials because smaller and more homogeneously fillers have been identified in CS (Fig. 8) and the material with the lowest surface reflectance.

The determined linear absorption coefficient indicates that GB (0.369 mm^{-1}) attenuates the incident irradiation stronger, while TC (0.281 mm^{-1}) was the most transparent material to radiation. This can be related to the high filler amount described in GB (86 wt. %) and the type of filler it contains. Although a detailed description of the chemical composition of the fillers is missing so far, fillers are referred by the manufacturer as ceramics. This suggests a higher refractive index of the fillers than regular glasses contained in resin composites. Consequently, mismatching between the refractive index of the filler and methacrylate matrix may occur, with the consequence of enhanced light scattering [20,21] and a higher linear absorption coefficient. The lowest linear absorption coefficient has not been identified in SB, the material with the lowest filler amount, but in TC, a material containing filler made of barium-aluminum-silicate glass with a mean particle size lower than 1 µm and silicon dioxide with a mean particle size lower than 20 nm (Fig. 8 and manufacturer information). Comparing only materials with a similar chemical composition of fillers (Silica and barium glass) and similar filler size and shape (Fig. 8), the linear absorption coefficient increases with the filler amount in the sequence BC > CS > TC. Note that SB, the material with the lowest filler amount (61%), contains spherical filler particles ranging between 1.0 and 10.0 µm (Fig. 8). It showed a similar linear absorption coefficient to CS, a material with a much higher filler amount (71%). This fact must be attributed to an increased scattering in SB, owing to the chemical composition of the fillers (Silica, silicate, zirconium silicate) containing elements of higher atomic number.

The linear absorption coefficient was not changed during aging in

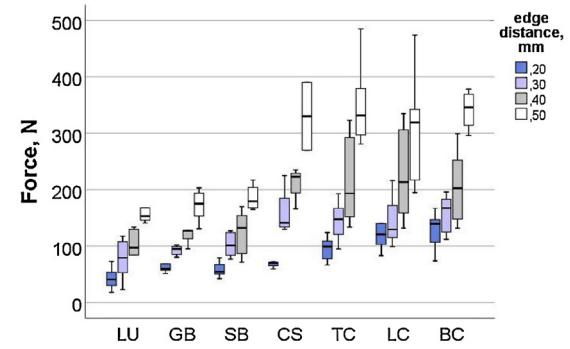

a)

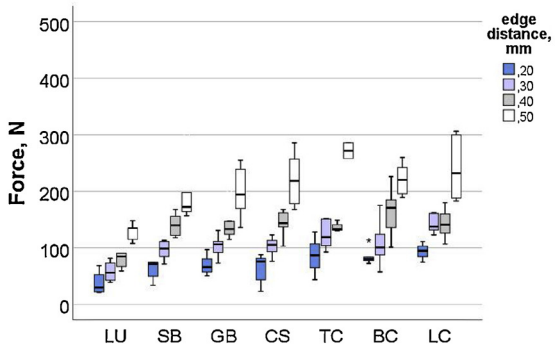

b)

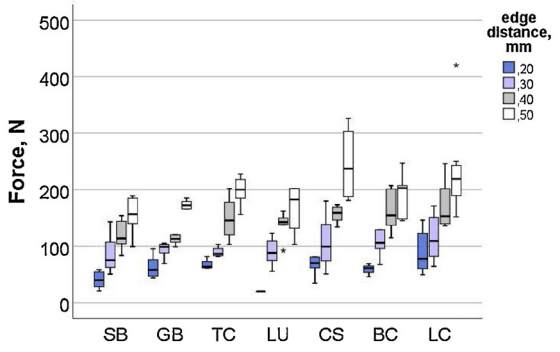

c)

Fig. 4. Edge force as a function of material measured on aging conditions a) no aging; b) thermo cycled (TC), c) storage in alcohol (ALC).

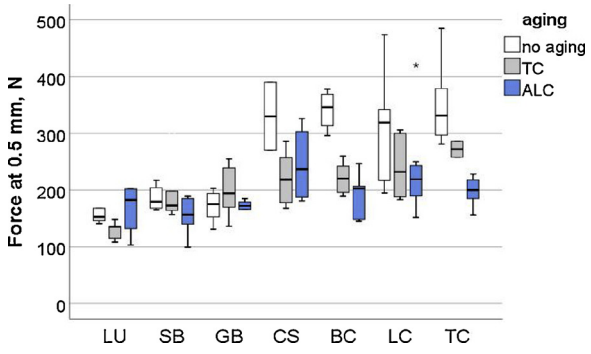

Fig. 5. Edge force at a chipping distance of 0.5 mm as a function of material and aging conditions.

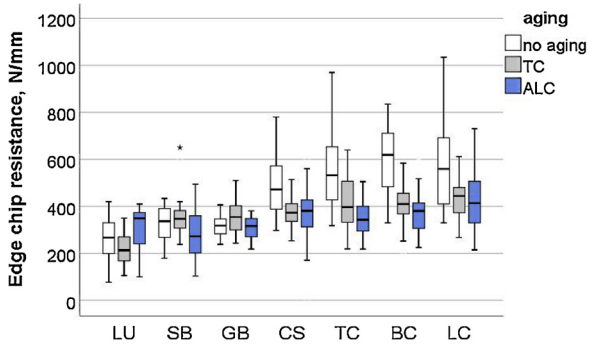

Fig. 6. Edge chip resistance as a function of material and aging.

Table 3
Effect of aging, material and their binary interaction product on the measured micro-mechanical properties: partial eta-squared values, η_p^2 ($p < 0.05$).

Parameter	Y	HM	HV	Cr	W_{elast}	W_{tot}
aging	0.864	0.883	0.879	0.819	0.768	0.863
material	0.991	0.988	0.984	0.94	0.988	0.984
aging * material	0.305	0.26	0.299	0.207	0.628	0.541

almost all of the analyzed materials. The above-described lowering in surface reflectance during aging may be related to surface altering. Because the incident light remains constant during all measurements, this result may translate to a decrease in reflected light during aging, a plausible indicator that the surface becomes rougher. Therefore, the reflectance likely determined by spectrometric analysis may serve as a convenient criterion for preliminary evaluation of surface degradation during aging. The fastest reduction in surface reflectance with aging, related to the control (non-aged) specimens, was identified in BC after thermocycling (21%, non-aged; 16% TC and 13% ALC) and in SB, after storage in alcohol (20%, non-aged; 18% TC and 11% ALC). This behavior cannot be related to the measured mechanical properties. Therefore, the reasons may only be speculative because no information is available regarding the type of monomers, initiators or chemical composition and stability of the silanes used to couple the fillers in the organic matrix. Both the chemical composition and filler size differ consistently among the mentioned materials (Fig. 8, Table 1).

As previously shown by Watts and Cash [17], to fit the Beer-Lambert law to the transmission of light through resin composites, allowance must be made for the surface reflection of incident radiation. Thus, the present study proposes further correction that allows calculating the true value of the transmitted irradiance through a material (I_t) from the measured spectrometer data ($I_{t,\ measured}$) as $I_t = I_{t,\ measured}/(1\text{-}R/2)$) with R = reflectance. Note that the difference between the true and measured values decreases exponentially with specimen thickness and was in the range of 68.2 mW/cm² (CS) to 108.35 (GB) mW/cm² in 0.5-mm-thick specimens: 20.35 mW/cm² (CS) to 29.48 mW/cm² (LU) in 2-mm-thick specimens and 5.17 mW/cm² (GB) to 7.96 mW/cm² (TC) in 4-mm-thick non-aged specimens. In a clinical situation, the underlying luting resin composite, wetting the restoration, may receive more light as usually indicated through spectroscopic valuations. This aspect may be of value in thin and more translucent restorations but will have less clinical relevance for thicker, more opaque ones.

Several mechanical properties of CAD/CAM resin composites were shown to degrade during aging [1,6]. This fact was confirmed by the present study, while the determined micromechanical parameters by depth-sensing indentation proved to be more sensitive to aging than the edge chipping resistance parameters. The aging protocols employed in the present study concerned thermal aging while subjecting the specimens to 10,000 thermocycles between 5 °C and 55 °C. This was estimated to represent approximately one year of clinical function [22].

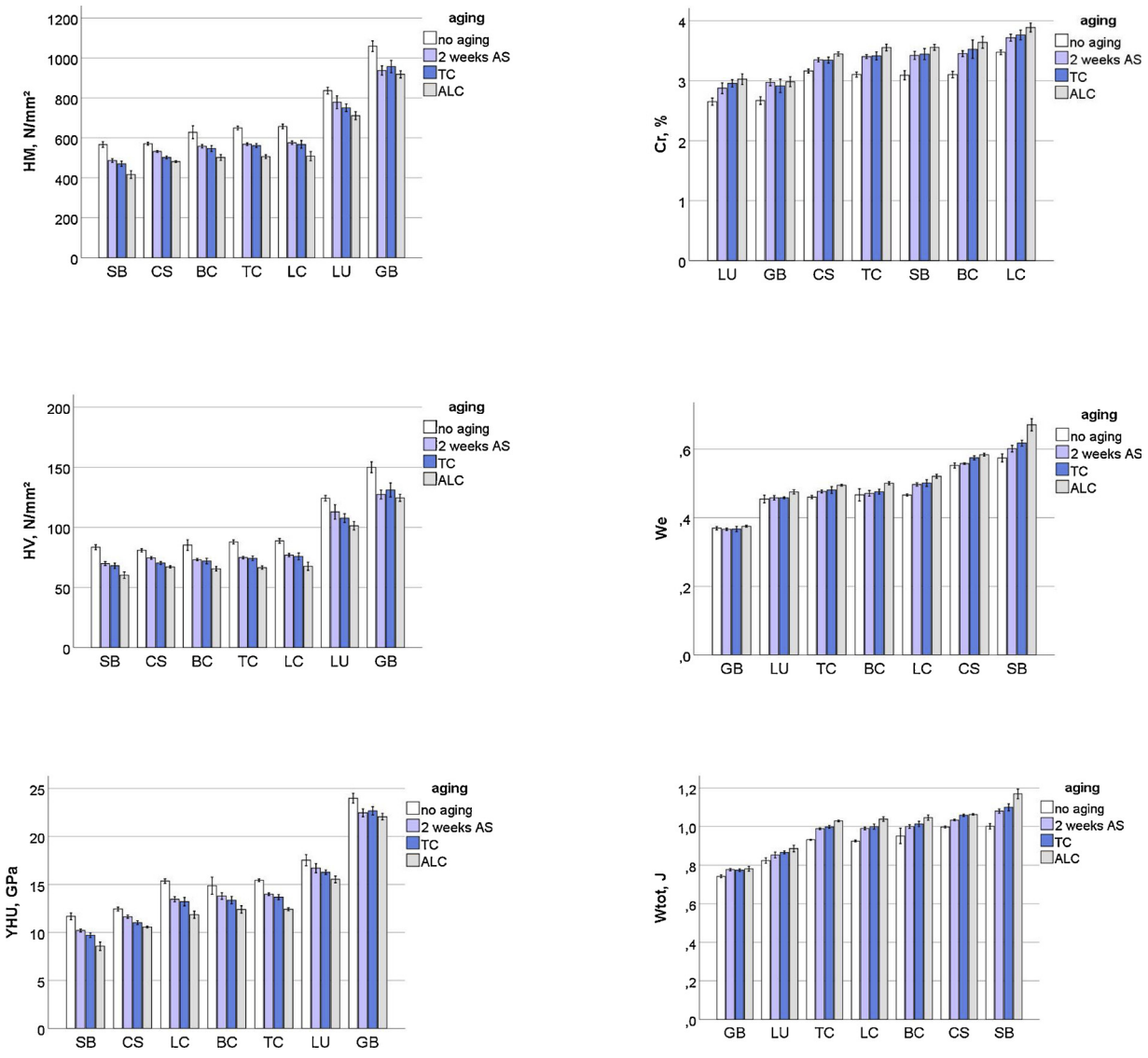

Fig. 7. Micro-mechanical properties (HM, HV, Y_{HU}, Cr, W_e, W_{tot}) as a function of material and aging.

Subsequent aging by storage in 75 vol. % alcohol/water solution was chosen based on previous correlation analysis of mechanical properties determined in vitro in regular resin composites and their clinical outcome. It has been identified that, when aging in ethanol, the flexural strength decrease is correlated very strongly with the clinical index [23].

Chipping from concentrated overloads is an important aspect for the edge integrity and survival of restorations made out of brittle materials [24]. An edge chipping test was therefore used to measure the fracture resistance of the analyzed CAD/CAM resin composites. The determined edge chipping resistance parameters identified a consistently stronger effect of the used restorative material than aging. However, it must be considered that the force-load location showed a nonlinear dependency, confirming the data described previously [7]. For routine evaluations and comparative purposes, two parameters were identified as suitable—the critical force to induce a chip at a 0.5-mm edge distance, which is considered a clinically relevant chipping distance, and the edge chip resistance [7]. The measured values for the critical force to induce a chip at a 0.5-mm edge distance are in the same range with values described by Quinn [7] for resin composites or by Pfeilschifter et al. for CAD/CAM resin composites [12]. However, it should be noted that data scattering was consistently larger in the present study than data published by Quinn [7] but lower than or comparable to recently published data [12]. Whether this can be attributed to the higher loading velocity (1 mm/min and 3 mm/min [7] vs. 0.5 mm/min) or to the detection of the chipping load by the more accurate acoustic method [7] needs to be further analyzed.

With the limitation of the low products available for comparison in the current literature, the determined edge chipping resistance parameters on simple rectangular test blocks showed a similar ranking to fracture loads measured on crowns [25] made of the same materials (CS > SB). Additionally, the probability of fracture after thermal aging was higher in CS (24.6% and 14% respectively) [25].

The measurement of the micromechanical properties involves an additional intermediate stage that assessed the material properties directly after storage in artificial saliva and thus prior to TC. This additional measurement revealed a marked weakening of all micromechanical properties already after moister storage, while subsequent aging by TC maintained or decreased the properties only slightly. The replacement of water by ethyl alcohol solution (whose individual plasticizing action is more efficient) in the subsequent aging step leads to an additional reduction in all micromechanical properties, except for GB. This was related to the high filler load and, hence, lower polymer content prone to plasticization. The lower mechanical properties after aging identified in SB, compared with CS and BC, as well as the identified differences in filler size (Fig. 8), may be well corroborated with

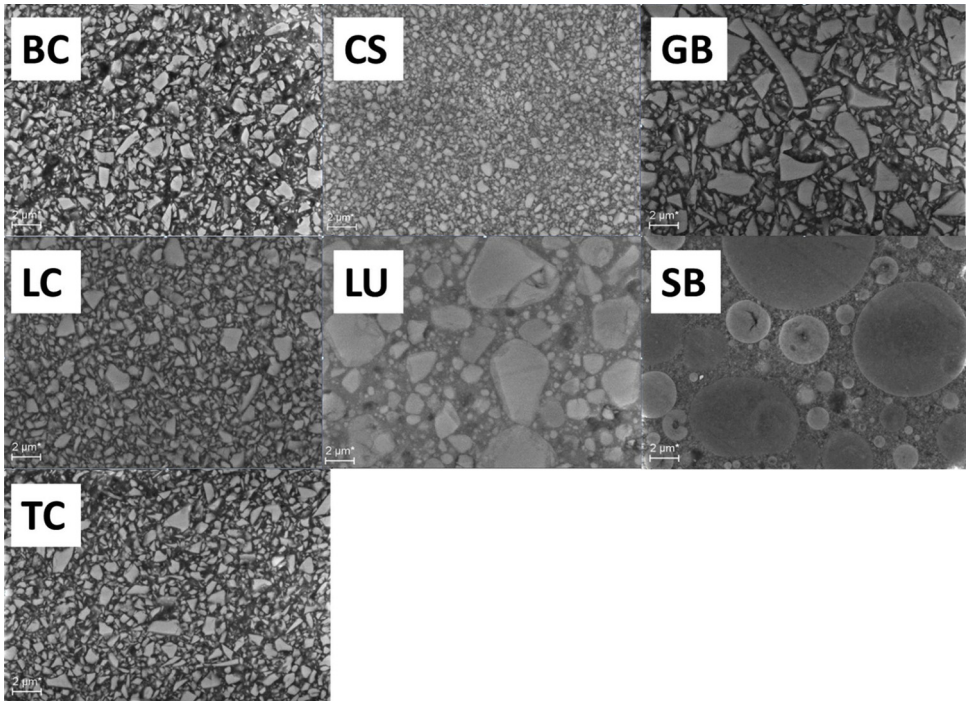

Fig. 8. Scanning electron microscopy (SEM) on unsputtered specimens.

previously published data that measured SB at a higher volume loss than that of CS and BC using a 2-body wear test instead of human enamel antagonists [26]. It is noteworthy that, in non-aged specimens of SB, CS, and BC, the measured micromechanical properties were comparable, emphasizing the importance of considering aging in this type of evaluation. Moreover, it has been previously published that CAD/CAM resin composite crowns would have sufficient strength to withstand the bite force of the molar teeth (700–900 N) [27].

5. Conclusions

A definite relationship exists between true and measured irradiance: the thinner and more translucent the specimen is, the greater is the failure. For the analyzed high-translucent CAD/CAM resin composites and a clinically relevant restorative thickness of 2 mm, the discrepancy between the true and measured transmitted irradiance was estimated at 20.35 mW/cm^2 (CS) to 29.48 mW/cm^2 (LU).

The reflectance determined by spectrometric analysis was identified as a possible criterion to estimate the surface degradation during aging, while the linear absorption coefficient was generally maintained during aging. In all materials, the determined mechanical properties degraded during aging, while the micromechanical parameters determined by depth-sensing indentation reflected a more sensitive aging degradation than the edge chipping resistance parameters. It is also apparent that the filler amount and, consequently, the polymer amount, correlate very well with the determined micromechanical parameters, while the correlation even improves during aging. This statement is, however, not true for the determined chipping resistance parameters. All null hypotheses are therefore rejected.

Conflicts of interest statement

Author declares no conflict of interest.

Acknowledgements

The author kindly acknowledges the companies Coltene, GC, Voco, DMG, 3 M, Shofu and Ivoclar Vivadent for providing the CAD-CAM resin composits used in the present study. No fundings have been received.

References

[1] N.D. Ruse, M.J. Sadoun, Resin-composite blocks for dental CAD/CAM applications, J. Dent. Res. 93 (12) (2014) 1232–1234.
[2] S. Ankyu, K. Nakamura, A. Harada, G. Hong, T. Kanno, Y. Niwano, U. Ortengren, H. Egusa, Fatigue analysis of computer-aided design/computer-aided manufacturing resin-based composite vs. lithium disilicate glass-ceramic, Eur. J. Oral Sci. 124 (4) (2016) 387–395.
[3] F.A. Shembish, H. Tong, M. Kaizer, M.N. Janal, V.P. Thompson, N.J. Opdam, Y. Zhang, Fatigue resistance of CAD/CAM resin composite molar crowns, Dent. Mater. 32 (4) (2016) 499–509.
[4] N.C. Lawson, R. Bansal, J.O. Burgess, Wear, strength, modulus and hardness of CAD/CAM restorative materials, Dent. Mater. 32 (11) (2016) e275–e283.
[5] B. Hussain, M.K.L. Thieu, G.F. Johnsen, J.E. Reseland, H.J. Haugen, Can CAD/CAM resin blocks be considered as substitute for conventional resins? Dent. Mater. 33 (12) (2017) 1362–1370.
[6] T.S. Porto, R.C. Roperto, A. Akkus, O. Akkus, S. Teich, F. Faddoul, S.T. Porto-Neto, E.A. Campos, Effect of storage and aging conditions on the flexural strength and flexural modulus of CAD/CAM materials, Dent. Mater. J. (2018).
[7] G.D. Quinn, On edge chipping testing and some personal perspectives on the state of the art of mechanical testing, Dent. Mater. 31 (1) (2015) 26–36.
[8] ASTM WK45217, Draft Standard Test Method for Resistance to Edge Chipping of Brittle Materials, Committee C-28 Advanced Ceramics, ASTM International, West Conshohocken, PA, USA, 2014.
[9] CEN Standard, European Prestandard, prTS 843-9, Advanced Technical Ceramics – Mechanical Properties of Monolithic Ceramics at Room Temperature, Part 9: Method of Test for Edge-chip Resistance, European Standard Committee TC 184, Brussels, 2009.
[10] H. Chai, J.J. Lee, B.R. Lawn, On the chipping and splitting of teeth, J. Mech. Behav. Biomed. Mater. 4 (3) (2011) 315–321.
[11] G.D. Quinn, A.A. Giuseppetti, K.H. Hoffman, Chipping fracture resistance of denture tooth materials, Dent. Mater. 30 (5) (2014) 545–553.
[12] M. Pfeilschifter, V. Preis, M. Behr, M. Rosentritt, Edge strength of CAD/CAM materials, J. Dent. 74 (2018) 95–100.
[13] G.D. Quinn, A.A. Giuseppetti, K.H. Hoffman, Chipping fracture resistance of dental CAD/CAM restorative materials: part I–procedures and results, Dent. Mater. 30 (5) (2014) e99–e111.
[14] D.C. Watts, M. Issa, A. Ibrahim, J. Wakiaga, K. Al-Samadani, M. Al-Azraqi, N. Silikas, Edge strength of resin-composite margins, Dent. Mater. 24 (1) (2008) 129–133.
[15] H. Chai, X. Wang, J. Sun, Miniature specimens for fracture toughness evaluation of dental resin composites, Dent. Mater. (2018).
[16] Y. Zhang, J.J. Lee, R. Srikanth, B.R. Lawn, Edge chipping and flexural resistance of monolithic ceramics, Dent. Mater. 29 (12) (2013) 1201–1208.
[17] D.C. Watts, A.J. Cash, Analysis of optical transmission by 400-500 nm visible light

into aesthetic dental biomaterials, J. Dent. 22 (2) (1994) 112–117.
[18] C.P. Turssi, J.L. Ferracane, K. Vogel, Filler features and their effects on wear and degree of conversion of particulate dental resin composites, Biomaterials 26 (24) (2005) 4932–4937.
[19] J. Da Costa, J. Ferracane, R.D. Paravina, R.F. Mazur, L. Roeder, The effect of different polishing systems on surface roughness and gloss of various resin composites, J. Esthet. Restor. Dent. 19 (4) (2007) 214–224 discussion 225-6.
[20] W.M. Palin, J.G. Leprince, M.A. Hadis, Shining a light on high volume photocurable materials, Dent. Mater. 34 (5) (2018) 695–710.
[21] A.C. Shortall, W.M. Palin, P. Burtscher, Refractive index mismatch and monomer reactivity influence composite curing depth, J. Dent. Res. 87 (1) (2008) 84–88.
[22] M.S. Gale, B.W. Darvell, Thermal cycling procedures for laboratory testing of dental restorations, J. Dent. 27 (2) (1999) 89–99.
[23] S.D. Heintze, N. Ilie, R. Hickel, A. Reis, A. Loguercio, V. Rousson, Laboratory mechanical parameters of composite resins and their relation to fractures and wear in clinical trials-A systematic review, Dent. Mater. 33 (3) (2017) e101–e114.
[24] K.J. Anusavice, K. Kakar, N. Ferree, Which mechanical and physical testing methods are relevant for predicting the clinical performance of ceramic-based dental prostheses? Clin. Oral Implants Res. 18 (Suppl 3) (2007) 218–231.
[25] S. Yamaguchi, R. Kani, K. Kawakami, M. Tsuji, S. Inoue, C. Lee, W. Kiba, S. Imazato, Fatigue behavior and crack initiation of CAD/CAM resin composite molar crowns, Dent. Mater. (2018).
[26] C. Stockl, R. Hampe, B. Stawarczyk, M. Haerst, M. Roos, Macro- and micro-topographical examination and quantification of CAD-CAM composite resin 2- and 3-body wear, J. Prosthet. Dent. (2018).
[27] R. Okada, M. Asakura, A. Ando, H. Kumano, S. Ban, T. Kawai, J. Takebe, Fracture strength testing of crowns made of CAD/CAM composite resins, J. Prosthodont. Res. 62 (3) (2018) 287–292.